# Nonlinear Control for Bidirectional Power Converter in a dc Microgrid ⋆

**Eduardo Lenz** * **Daniel J. Pagano** *

* *Department of Automation and Systems, Federal University of Santa Catarina, Florianópolis, Brazil (e-mail: {edulenz,daniel}@das.ufsc.br)*

**Abstract:** Some comparative studies of several nonlinear control techniques applied to dc-dc power converters are developed in this paper, like for instance the Immersion & Invariance, Passivity-Based Control, Feedback Linearization and the Sliding-Mode Control. All these different control strategies are used to drive dc-dc power converters in a dc microgrid. The load, modeled as a Constant Power Load type, is also a major issue of this paper.

Keywords: Immersion & Invariance; Feedback Linearization; Sliding-mode Control; Passivity-based Control; Microgrids; Constant Power Loads; dc-dc Power Converters.

## 1. INTRODUCTION

The purpose of this paper is to apply several nonlinear control techniques to drive a bidirectional dc-dc power converter, which is part of a microgrid, and compare each technique through simulation results. The techniques we are interested in are the Passivity-Based Control (PBC), the Immersion & Invariance (I&I), Feedback Linearization (FL) and the Sliding-Mode Control (SMC).

Feedback Linearization is a classical control strategy, but suffers some criticism for two main reasons: (i) it lacks robustness with respect to uncertain parameters; (ii) it destroys every nonlinear phenomenon even if it is a beneficial one. We are going to fix the first problem by using the I&I (Astolfi and Ortega [2003]) as an nonlinear estimation for the uncertain parameters. Naturally, the second item is the core of the technique and cannot be changed.

Usually in power electronics the control system is divided in two loops: (i) the inner loop, which controls the inductor current; and (ii) the outer loop, which controls the capacitor voltage. For the inner loop, the FL and PBC will be compared, with both having nonlinear estimation incorporated through the I&I technique. In the case of the outer loop, only the I&I will be used. Note that this division on the control strategy must obey some basic rules: the inner loop must be faster than the outer loop; and from this consideration the outer loop only sees the steady state operation of the inner loop dynamics.

In the case of the SMC, the situation is a little bit different. There is only one control loop, where the inductor current and the capacitor voltage are measured and used to generate the PWM signals necessary to drive the switches in a power converter.

The bidirectional dc-dc power converter (the main object of study in this paper) is part of a microgrid (Boroyevich et al. [2010]). A microgrid is an electrical distribution system that operates with or without the main grid (either connected or isolated) and have several sources (auxiliary) and loads. These auxiliary sources are renewable sources, because of the modern concern about the environment. In our example, the microgrid operates in isolated mode (islanded) and have two sources and two loads (Fig. 1). The components are: a photovoltaic panel (PV) as the renewable energy source; one resistive load; a Constant Power Load (CPL) made by a dc-dc power converter with a resistive load; and a dc-dc bidirectional power converter connected to a battery. The objective of the bidirectional dc-dc power converter is to regulate the dc link voltage despite the interactions of all the sources and loads.

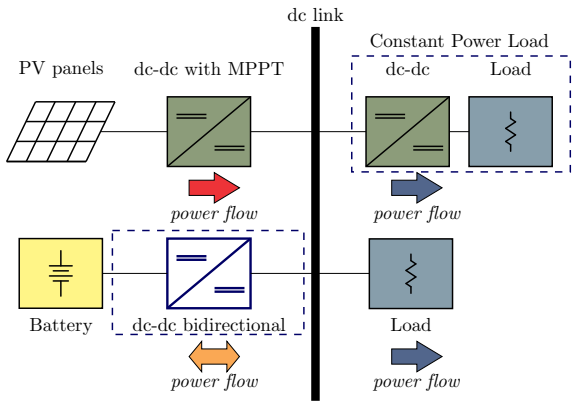


Fig. 1. The dc microgrid.

CPL (Kwasinski and Krein [2007], Onwuchekwa and Kwasinski [2010], Zhang and Yan [2011]) are models that incorporate the effects of a control loop in a power converter when this converter is viewed as a load (or even as a source). This component could be a cause of instability in the dc link voltage due to its negative resistance feature, when it is linearized. In our case, the components that are CPL-types are the renewable source and the load driven by a dc-dc power converter.

⋆ Project developed under the R&D Program of Tractebel Energia regulated by ANEEL.

 

## 2. DC-DC BIDIRECTIONAL POWER CONVERTER

The equivalent structure of the microgrid with the components replaced by ideal sources is given in Fig. 2 and the topology of the bidirectional dc-dc power converter is shown in Fig. 3. All the loads and sources (besides the battery) are modeled as a CPL ($P_{\rm dc} = P_{\rm S} + P_{\rm L}$) connected in parallel to a resistive load. As the renewable source is operating in the Maximum Power Point Tracking (MPPT), for steady weather conditions we can model this source as a CPL (with a reverse signal).

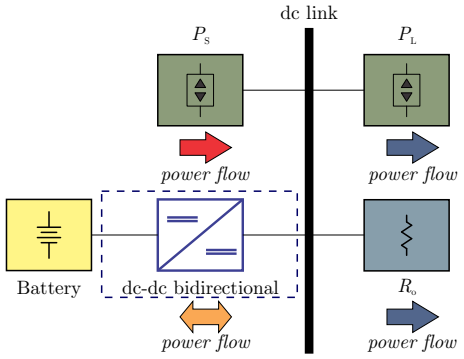


Fig. 2. Equivalent microgrid structure.

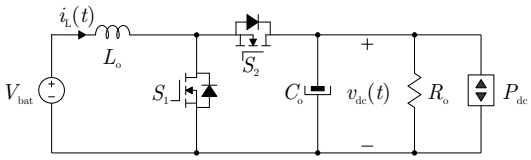


Fig. 3. Topology of the bidirectional dc-dc power converter.

The bidirectional power flow capability of the power converter is due to the presence of two transistors (with diodes in parallel) instead of using one active switch and one passive switch (a diode). As the focus is on the dc link voltage control, the battery is assumed to be ideal and the charging procedure will not be pursued.

The equivalent load characteristic, connected to the bidirectional power converter, is presented in Fig. 4. Because some CPL have different power flow directions, the load curves were generated for both positive and negative power flows. Also, the slight difference between the curves occurs because of variations on the load resistance. It is possible to see that, depending on values of $P_{\rm dc}$ and $R_{\rm o}$, the prevailing load type can be a CPL or a resistive one. One important remark: when the load operates with low voltage, the current will not go to infinity as one may think. With low voltage a true CPL behaves as a resistive load or even as a constant current (that depends on the circuit topology and its control). The power converter operates in this region only in the start up and possibly when the system protection enters.

The local average model of the bidirectional power converter is given by

$$L_{\rm o}\frac{di_{\rm L}}{dt} = -\left(1-u\right)v_{\rm dc} + V_{\rm bat} \tag{1}$$

$$C_{\rm o}\frac{dv_{\rm dc}}{dt} = \left(1-u\right)i_{\rm L} - i_{\rm dc} \tag{2}$$

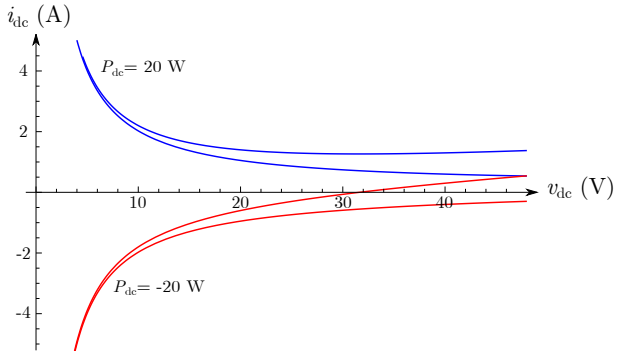


Fig. 4. Idealized equivalent load connected to the dc link.

where

$$i_{\rm dc} = \frac{P_{\rm dc}}{v_{\rm dc}} + \frac{v_{\rm dc}}{R_{\rm o}}; \tag{3}$$

$i_{\rm L}$ and $v_{\rm dc}$ are the states of the system; $V_{\rm bat}$ is the battery voltage; $u$ is the duty cycle; and $i_{\rm dc}$ is the dc link current. $L_{\rm o}$ is the inductance; $C_{\rm o}$ is the capacitance; $P_{\rm dc}$ and $R_{\rm o}$ are the load parameters and the control variable is limited to the following interval: $u \in [0; 1]$.

Although we can model the load seen by the bidirectional power converter as the sum of a resistive and a CPL, we are going to assume that the resistive part is negligible when compared to the CPL (by comparing the consumed power of both loads for the rated dc link voltage). This choice reflects the more modern tendency of loads connected to the dc link through a power converter with a control loop. Therefore the control design will focus only on the CPL, but in our simulations both kind of loads will be used. Even if the resistive part prevails over the CPL the control system will work properly.

Besides the load modeling it is important to obtain a normalized model for the bidirectional power converter, thus (1) and (2) become

$$\dot{x}_1 = -\left(1-u\right)x_2 + E_{\rm bat} \tag{4}$$

$$\dot{x}_2 = \left(1-u\right)x_1 - \frac{p_{\rm o}}{x_2} \tag{5}$$

where $x_1 = \left(Z_{\rm o}/V_{\rm n}\right)i_{\rm L}$; $x_2 = v_{\rm dc}/V_{\rm n}$; $E_{\rm bat} = V_{\rm bat}/V_{\rm n}$; $\tau = \omega_{\rm o}t$; $p_{\rm o} = \left(Z_{\rm o}/V_{\rm n}^2\right)P_{\rm dc}$; $Z_{\rm o} = \sqrt{L_{\rm o}/C_{\rm o}}$; $\omega_{\rm o} = 1/\sqrt{L_{\rm o}C_{\rm o}}$; and $V_{\rm n}$ is the rated input (battery) voltage. Note that the differentiation is about $\tau$.

## 3. PASSIVITY-BASED CONTROL AND IMMERSION & INVARIANCE CONTROL

### *3.1 Inner Loop*

The PBC design is easily done for the bidirectional power converter and is given by

$$\dot{z}_1 = -\left(1-u\right)z_2 + E_{\rm bat} + \mathcal{K}_1\left(x_1 - z_1\right) \tag{6}$$

$$\dot{z}_2 = \left(1-u\right)z_1 - \frac{\hat{p}_{\rm o}}{z_2} + \mathcal{K}_2\left(x_2 - z_2\right) \tag{7}$$

where $z_1$ is the control variable that represents the current ($x_1$); in the same way $z_2$ represents the output voltage ($x_2$); $\mathcal{K}_1$ and $\mathcal{K}_2$ are the gains of the controller; and $\hat{p}_{\rm o}$ is an estimation of the power processed by the converter.

The PBC will be used to control the current in the bidirectional power converter ($x_1$). The output voltage ($x_2$) will be controlled by the I&I control. As the PBC is a current-mode control, the $z_1$ variable is actually the reference signal for the inner loop, generated by the outer loop (I&I). $z_1$ can be approximated to a constant as both loops are decoupled by their time constants. The duty cycle is found by making (6) equal to zero:

$$u = 1 - \frac{E_{\text{bat}} + \mathcal{K}_1 (x_1 - z_1)}{z_2}. \tag{8}$$

The estimation of $p_{\text{o}}$ is developed through the I&I scheme. Defining the error of the parameter as

$$z_p = \alpha_p + \beta_p (x_2) - p_{\text{o}} \tag{9}$$

and assuming that $p_{\text{o}}$ is constant (as there is no problem for a slow variation), the error dynamics is given by

$$\dot{z}_p = \dot{\alpha}_p + \frac{\partial \beta_p}{\partial x_2} \left[ (1-u) x_1 - \frac{(\alpha_p + \beta_p - z_p)}{x_2} \right]. \tag{10}$$

Choosing $\dot{\alpha}_p$ to cancel all terms other than $z_p$ in (10), we have

$$\dot{z}_p = \frac{\partial \beta_p}{\partial x_2} \frac{z_p}{x_2}. \tag{11}$$

With $\partial \beta_p / \partial x_2 = -\gamma x_2^3$, $\beta_p$ is given by

$$\beta_p = -\frac{1}{4} \gamma x_2^4 \tag{12}$$

where $\gamma$ is a constant parameter. With this choice of $\beta_p$, $z_p$ is asymptotically stable ($\dot{z}_p = -\gamma x_2^2 z_p$), thus we can replace $p_{\text{o}}$ by $\alpha_p + \beta_p$. Finally, $\dot{\alpha_p}$ is found to be

$$\dot{\alpha_p} = \gamma x_2^2 \big[ (1-u) x_1 x_2 - \alpha_p - \beta_p \big]. \tag{13}$$

Now every parameter in (6) and (7) is known (note that $\hat{p}_{\text{o}} = p_{\text{o}}$) and we can proceed to proof that $x_1$ will follow $z_1$ and therefore show that the system is stable. Using the proposed Lyapunov function

$$\mathcal{V} = \frac{1}{2} (x_1 - z_1)^2 + \frac{1}{2} (x_2 - z_2)^2 \tag{14}$$

its dynamics is

$$\dot{\mathcal{V}} = -\mathcal{K}_1 (x_1 - z_1)^2 - \left( \mathcal{K}_2 - \frac{p_{\text{o}}}{x_2 z_2} \right) (x_2 - z_2)^2. \tag{15}$$

Although the system stability is not global, it is possible to find a value of $\mathcal{K}_2$ that stabilizes the system for a fixed $p_{\text{o}}$. For values greater than the rated one, the system protection is activated. Note that we have shown that the states of the converter will follow the control variables. We did not show that $z_2$ is a stable signal. Only with the outer loop we will achieve asymptotic stability.

The estimation of the output power ($p_{\text{o}}$) is not really important for this control, its use here is just to unburden the gains of the PBC so the errors between the PBC states and the power converter states are minimized. There are better ways to estimate this parameter, but it is out of the scope of this paper.

### *3.2 Outer Loop*

It is possible to make some approximations for the outer loop modeling, for instance: $(1-u) \cong E_{\text{bat}}/z_2$, since $z_2 \to x_2$ and $x_1 \to z_1$. So the converter dynamics becomes

$$\dot{x}_2 = \frac{E_{\text{bat}} z_1 - p_{\text{o}}}{x_2}. \tag{16}$$

By making a state transformation ($y_{\text{o}} = \frac{1}{2} x_2^2$) and noting that $p_{\text{in}} = E_{\text{bat}} z_1$, the outer loop dynamics becomes

$$\dot{y}_{\text{o}} = p_{\text{in}} - p_{\text{o}}. \tag{17}$$

The target error dynamics ($\epsilon_{\text{o}} = Y_r - y_{\text{o}}$) is

$$\dot{\epsilon}_{\text{o}} = -p_{\text{in}} + p_{\text{o}}. \tag{18}$$

where $Y_r$ is the reference signal for the outer loop.

If we choose $p_{\text{in}} = K_1 \epsilon_{\text{o}} + p_{\text{o}}$ the system would be asymptotically stable ($K_1$ is just the controller gain), but $p_{\text{o}}$ is unknown, so to overcome this problem we are going to apply the I&I concepts through the following manifold

$$\mathcal{M} = \Big\{ (y_{\text{o}}, \alpha) \in \mathbb{R} \times \mathbb{R} \mid \alpha + \beta (y_{\text{o}}) - p_{\text{o}} = 0 \Big\} \tag{19}$$

and force it to be attractive. The off-dynamics manifold is

$$\dot{z} = \dot{\alpha} + \frac{\partial \beta}{\partial y_{\text{o}}} \Big[ p_{\text{in}} - \alpha - \beta + z \Big] \tag{20}$$

$$= \frac{\partial \beta}{\partial y_{\text{o}}} z \tag{21}$$

where in (21) $\dot{\alpha}$ was defined to cancel all terms other than $z$ in (20). With $\beta$ defined as

$$\beta = -\frac{1}{2} \lambda y_{\text{o}}^2 \tag{22}$$

$z$ becomes asymptotically stable:

$$z = z(0) \exp \left( -\lambda \int y_{\text{o}} (\tau) \, d\tau \right). \tag{23}$$

Therefore $p_{\text{o}} = \alpha + \beta$. $\lambda$ is a constant parameter linked with the convergence of the estimation of $p_{\text{o}}$. With $p_{\text{in}}$ replaced by $K_1 \epsilon_{\text{o}} + \alpha + \beta$, $\dot{\alpha}$ becomes

$$\dot{\alpha} = \lambda K_1 \epsilon_{\text{o}} y_{\text{o}} \tag{24}$$

and the output equation of the outer loop is

$$p_{\text{in}} = K_1 \epsilon_{\text{o}} + \lambda K_1 \int y_{\text{o}} (\tau) \, \epsilon_{\text{o}} (\tau) \, d\tau - \frac{\lambda}{2} y_{\text{o}}^2. \tag{25}$$

It turns out that this controller is similar to a PI control. Note that in the beginning, the error dynamics was chosen to be first order, but we could force a second order dynamics as well:

$$\dot{\epsilon}_{\text{o}} = -K_1 \epsilon_{\text{o}} - K_2 \int \epsilon_{\text{o}} (\tau) \, d\tau. \tag{26}$$

With this change and using the same $\beta$, (24) becomes

$$\dot{\alpha} = \lambda y_{\text{o}} \left[ K_1 \epsilon_{\text{o}} + K_2 \int \epsilon_{\text{o}} (\tau) \, d\tau \right] \tag{27}$$

and (25) changes to

$$p_{\text{in}} = K_1 \epsilon_{\text{o}} + \lambda K_1 \int y_{\text{o}} (\tau) \, \epsilon_{\text{o}} (\tau) \, d\tau - \frac{\lambda}{2} y_{\text{o}}^2 + K_2 \int \epsilon_{\text{o}} (\tau) \, d\tau + \lambda K_2 \int y_{\text{o}} (\tau) \int \epsilon_{\text{o}} (\xi) \, d\xi \, d\tau. \tag{28}$$

Note that $\xi$ was used as the dummy variable for the normalized time in the inner integral.

The output equation of the outer loop is

$$z_1 = \frac{p_{\text{in}}}{E_{\text{bat}}} \tag{29}$$

## 4. FEEDBACK LINEARIZATION CONTROL AND IMMERSION & INVARIANCE CONTROL

The combination of FL with the I&I will give the second approach to control the bidirectional power converter. The idea of using two loops to control the states ($x_1$ and $x_2$) will be the same of the PBC + I&I. Actually the whole outer loop scheme will be equal to what was done in the Section 3.2, the only difference being in the design of the inner loop.

The tracking error for the inner loop is

$$\epsilon_1 = X_r - x_1 \tag{30}$$

where $X_r$ is the reference for the inner loop (it is $z_1 = p_{\text{in}}/E_{\text{bat}}$ from Section 3.2). Deriving (30) until the control appears (assuming that $X_r$ is constant), we have

$$\dot{\epsilon}_1 = -\left[-\left(1-u\right)x_2 + E_{\text{bat}}\right]. \tag{31}$$

By choosing

$$u = \frac{x_2 + \nu - E_{\text{bat}}}{x_2} \tag{32}$$

the error dynamics is linearized:

$$\dot{\epsilon}_1 = -\nu. \tag{33}$$

We can set a first order or a second order dynamics for the error signal:

$$\nu = \mathcal{K}_1 \epsilon_1 \tag{34}$$

or

$$\nu = \mathcal{K}_1 \epsilon_1 + \mathcal{K}_2 \int \epsilon_1 \, d\tau. \tag{35}$$

The problem in linearizing the system is that it is necessary to know $E_{\text{bat}}$ exactly. To overcome this problem, the I&I scheme will be used to estimate the input voltage ($\hat{E} = \alpha_E + \beta_E$). The parameter error is equal to

$$z_E = \alpha_E + \beta_E\left(x_1\right) - E_{\text{bat}} \tag{36}$$

and its dynamics is (for a constant battery voltage)

$$\dot{z_E} = \dot{\alpha}_E + \frac{\partial \beta_E}{\partial x_1}\left[-\left(1-u\right)x_2 + \alpha_E + \beta_E - z_E\right] \tag{37}$$

$$= -\frac{\partial \beta_E}{\partial x_1} z_E. \tag{38}$$

The usual procedure of canceling everything except $z_E$ was made. By choosing

$$\beta_E = \frac{1}{3}\gamma x_1^3 \tag{39}$$

the error dynamics ($\dot{z}_E = -\gamma x_1^2 z_E$) becomes stable. Now it is possible to find $\dot{\alpha}_E$:

$$\dot{\alpha}_E = \gamma x_1^2 \nu. \tag{40}$$

The type of dynamic selected to $\nu$ affects the estimation of the parameter. The duty cycle with the estimation is

$$u = \frac{x_2 + \nu - \hat{E}}{x_2}. \tag{41}$$

Now we need to verify the internal dynamics stability. Because of the CPL, the system is unstable without a control loop for the output voltage. Therefore the I&I control developed in Section 3.1 will be used to show that the internal dynamics is stable. For the sake of simplicity, only the first order target dynamics will be developed.

Replacing (32) in (5), we have

$$\dot{x}_2 x_2 = x_1\left(E_{\text{bat}} - \nu\right) - p_{\text{o}}. \tag{42}$$

Using the same transformation ($y_{\text{o}} = \frac{1}{2}x_2^2$) used in the I&I control design and replacing (34) and (30) in (42), we have

$$\dot{y}_{\text{o}} = \epsilon_1\left(\mathcal{K}_1\epsilon_1 - \mathcal{K}_1 X_r - E_{\text{bat}}\right) + E_{\text{bat}} X_r - p_{\text{o}}. \tag{43}$$

Noting that

$$E_{\text{bat}} X_r = K_1\left(Y_r - y_{\text{o}}\right) + \hat{p}_{\text{o}} \tag{44}$$

and

$$\hat{p}_{\text{o}} - p_{\text{o}} \to 0 \tag{45}$$

$$\epsilon_1\left(\mathcal{K}_1\epsilon_1 - \mathcal{K}_1 X_r - E_{\text{bat}}\right) \to 0 \tag{46}$$

the internal dynamics is

$$\dot{y}_{\text{o}} = -K_1\left(y_{\text{o}} - Y_r\right). \tag{47}$$

Two practical remarks: (i) In the PBC, the battery voltage was also necessary to know, but the reason why the estimation was done only for the FL is because in the FL design the nonlinear terms are destroyed, unlike in the PBC. (ii) In the FL, there is a singularity in (32) when the output voltage is zero. When operating with low voltage, the duty cycle can be made equal to zero, thus increasing the output voltage until it is equal to the battery voltage (or just until it is in a safe value). In the case of the PBC it is easier to avoid such problem. The variable $z_2$ is determined by the PBC, so a nonzero initial value should be chosen.

## 5. SLIDE-MODE CONTROL

The SMC is a different kind of control, primary because it is applied to the converter instantaneous model rather than the averaged model. It is intended to operate in high frequency, although we can operate it with almost a low constant switching frequency (through a hysteresis band). The sampling frequency, however, needs to be higher than those used in the others controllers developed in this paper by at least an order of magnitude more. This is one of the drawbacks of this technique, but the simplicity of the controller design is a good advantage over the other options.

If we interpret (4) and (5) as the instantaneous states of the system and the duty cycle ($u$) as the PWM signal (a pulse that is zero or one), we can include a washout filter and the following switching surface to control the system:

$$\dot{x}_3 = \omega\left(x_1 - x_3\right) \tag{48}$$

$$h\left(\mathbf{x}\right) = \left(Y_r - x_2\right) - k\left(x_1 - x_3\right) \tag{49}$$

$$u = \frac{1}{2}\Big(1 + \text{sign}\left(h\right)\Big) \tag{50}$$

where $x_3$ is the filtered current.

The purpose of the washout filter (a high-pass filter) is to make the current not dependent on the load parameters. It is a similar logic to an integral control. The gradient for this sliding surface (49) is

$$\nabla h = \left[-k;\ -1;\ k;\right]. \tag{51}$$

If we write the state equation as

$$\dot{\mathbf{x}} = \mathbf{f}(\mathbf{x}, u) \tag{52}$$

then, when $u = 1$, (52) is equal to

$$\mathbf{f}_{\text{on}} = \begin{bmatrix} E_{\text{bat}} \\ -\dfrac{p_{\text{o}}}{x_2} \\ \omega(x_1 - x_3) \end{bmatrix} \tag{53}$$

and for $u = 0$

$$\mathbf{f}_{\text{off}} = \begin{bmatrix} E_{\text{bat}} - x_2 \\ x_1 - \dfrac{p_{\text{o}}}{x_2} \\ \omega(x_1 - x_3) \end{bmatrix}. \tag{54}$$

Now, we can calculate the inner product between (51) and (53); and also between (51) and (54).

$$\langle \nabla h, \mathbf{f}_{\text{on}} \rangle = -E_{\text{bat}} k + \frac{p_{\text{o}}}{x_2} + k\omega(x_1 - x_3) \tag{55}$$

$$\langle \nabla h, \mathbf{f}_{\text{off}} \rangle = -E_{\text{bat}} k + \frac{p_{\text{o}}}{x_2} + k\omega(x_1 - x_3) + kx_2 - x_1. \tag{56}$$

For switching action to occur it is necessary that $\langle \nabla h, \mathbf{f}_{\text{on}} \rangle < 0$ and $\langle \nabla h, \mathbf{f}_{\text{off}} \rangle > 0$, thus $k$ must be chosen to match these conditions.

In the sliding regime ($h = 0$), the converter becomes a second-order system:

$$\mathbf{f}_s = \begin{bmatrix} \dfrac{(p_{\text{o}} - E_{\text{bat}} x_1) + \omega(Y_r - x_2) x_2}{kx_2 - x_1} \\ \dfrac{-k(p_{\text{o}} - E_{\text{bat}} x_1) - \omega(Y_r - x_2) x_1}{kx_2 - x_1} \end{bmatrix} \tag{57}$$

$\mathbf{f}_s$ is the sliding vector field.

The jacobian matrix of the system is

$$\mathbf{J} = \frac{1}{Y_r k - \dfrac{p_{\text{o}}}{E_{\text{bat}}}} \begin{bmatrix} -E_{\text{bat}} & -\omega Y_r \\ E_{\text{bat}} k & \omega \dfrac{p_{\text{o}}}{E_{\text{bat}}} \end{bmatrix}. \tag{58}$$

The values of $k$ and $\omega$ to ensure stability of the system in the sliding regime using standard stability analysis are

$$k > \frac{p_{\text{o}}}{Y_r E_{\text{bat}}} \tag{59}$$

$$\omega < \frac{E_{\text{bat}}^2}{p_{\text{o}}}. \tag{60}$$

More details about Washout-SMC applied to dc-dc power converters can be found in Pagano and Ponce [2009] and Tahim et al. [2012].

## 6. SIMULATION RESULTS

The system specification is shown in Table 1.

The control configurations that will be analyzed here are:

- Second order dynamics for the FL and first order dynamics for I&I (FL 2 + I&I 1)
- Second order dynamics for both FL and I&I (FL 2 + I&I 2)
- PBC and first order dynamics for the I&I (PBC + I&I 1)
- PBC and second order dynamics for the I&I (PBC + I&I 2)
- SMC

Table 1. System Specification

| | |
|---|---|
| rated power | 20 W |
| input voltage | 24 V |
| output voltage | 48 V |
| switching frequency | 20 kHz |
| inductance | 2.2 mH |
| capacitance | 10 $\mu$F |

To analyze the system equilibrium point stability, several plots of the gains of the controllers will be presented. In the case of PBC, the stability can be seen in the ($\mathcal{K}_1$,$\mathcal{K}_2$)-plane (Fig. 5) for three levels of power. A similar graph is made for the FL (Fig. 6). In all cases, the increase of power shrinks the stable region.

As the duty cycle is limited, the system may enter in a saturation region and the control will not work. Note that each lower level of power includes the stable region of the higher level of power.

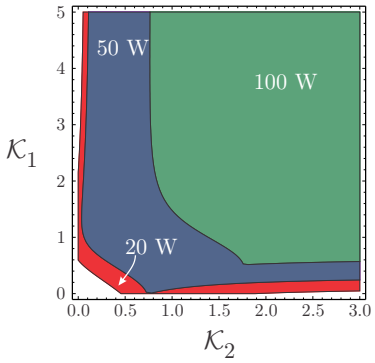


Fig. 5. The PBC controller region of stability.

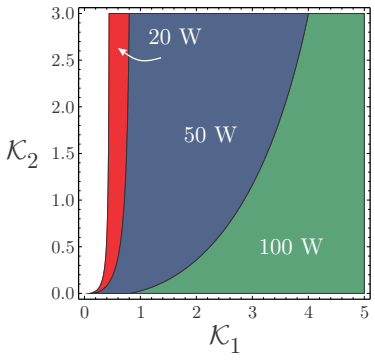


Fig. 6. The FL controller region of stability.

The waveforms of the dc link voltage in the transient regime, before the converter was pre-charged, are shown in Fig. 7 for all the combinations developed in the past sections; Fig. 8 shows the converter response for a input (battery) voltage of 20V; Fig. 9 presents the response of all control systems under reverse power flow condition; and

Fig. 10 shows that even for a predominant resistive load all controllers works well.

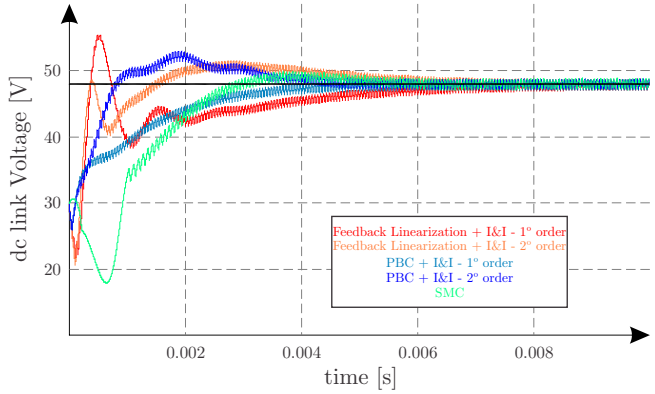


Fig. 7. Transient waveforms of the dc link voltage for PBC, FL and SMC.

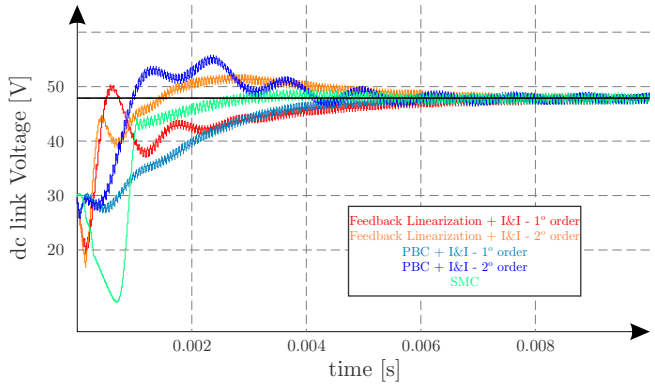


Fig. 8. Transient waveforms of the dc link voltage for a non rated battery voltage.

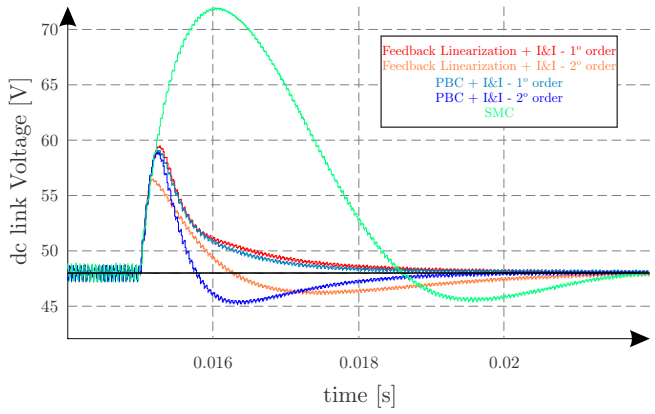


Fig. 9. dc link voltage for PBC, FL and SMC (for $0 < t < 0.015$ the power processed is 20W and for $t > 0.015$ is $-20$W).

Analyzing Fig. 7 we can see that the SMC has a significant undershoot and the FL 2 + I&I 1 got the biggest overshoot. PBC + I&I 1 and the FL 2 + I&I 2 were the controllers with the best transient response.

The SMC was by far the worst in the load transition (Fig. 9), higher overshoot and lower settling time. The lower overshoot was from the FL 2 + I&I 2. Besides the SMC all controllers had similar results.

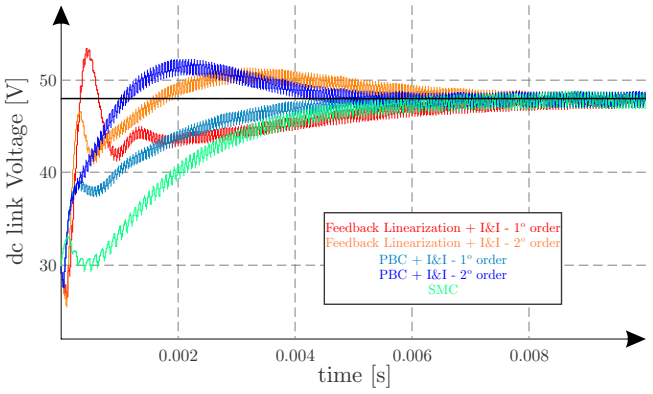


Fig. 10. Transient waveforms of the dc link voltage for a predominant resistive load.

In the case of a lower input voltage (Fig. 10), all control schemes work fine, even the FL where this parameter was estimated. For a resistive load, the controllers also track the reference signal without any trouble. Because of the nature of a resistive load, which increases damping, the waveforms have less oscillations.

## 7. CONCLUSION

All the control systems used in this paper achieved their purpose, i.e., to regulate the dc link voltage subject to changes in the load power. However, the best performance was obtained using the PBC with a first order dynamics I&I and the FL with a second order I&I. With the increase of power, all controllers will eventually reach an instability region, therefore it is essential that a protection circuit be present especially in a microgrid.

## REFERENCES

A. Astolfi and R. Ortega. Immersion and invariance: A new tool for stabilization and adaptive control of nonlinear systems. *IEEE Transactions on Automatic Control*, 48(4):590–606, 2003.

D. Boroyevich, I. Cvetkovic, D. Dong, R. Burgos, F. Wang, and F. Lee. Future electronic power distribution systems – a contemplative view. In *12th International Conference on Optimization of Electrical and Electronic Equipment (OPTIM)*, 2010.

A. Kwasinski and P.T. Krein. Stabilization of constant power loads in dc-dc converters using passivity-based control. In *29th International Telecommunications Energy Conference (INTELEC)*, pages 867–874, 2007.

C.N. Onwuchekwa and A. Kwasinski. Analysis of boundary control for buck converters with instantaneous constant-power loads. *IEEE Transactions on Power Electronics*, 25(8):2018–2032, 2010.

D. Pagano and E. Ponce. On the robustness of the dc-dc boost converter under washout smc. In *Brazilian Power Electronics Conference (COBEP)*, 2009.

A. Tahim, D. Pagano, and E. Ponce. Nonlinear control of dc-dc bidirectional converters in stand-alone dc microgrids. In *51st IEEE Conference on Decision and Control*, dec 2012.

F. Zhang and Y. Yan. Start-up process and step response of a dc–dc converter loaded by constant power loads. *IEEE Transactions on Industrial Electronics*, 58(1):298–304, 2011.